Optik 125 (2014) 6579–6585

Contents lists available at ScienceDirect

Optik

journal homepage: www.elsevier.de/ijleo

A new type of flight simulator for manual command to line-of-sight guided missile

Milos Pavic*, Slobodan Mandic, Danilo Cuk, Bojan Pavkovic

Military Technical Institute (VTI), Belgrade, Serbia

ARTICLE INFO

Article history:
Received 21 November 2013
Accepted 20 June 2014

Keywords:
Manual command to line-of-sight guidance
Antitank missile
Electro-optical sensors
Flight simulator

ABSTRACT

The manual command to line-of-sight guidance system of the antitank missiles requires a human operator in the guidance loop. His task is to track both the target and the missile and to generate commands in order to bring the missile into line-of-sight. The efficiency of the guidance depends on the skill of the human operator. A new type of training flight simulator for manual command to line-of-sight guidance, which realization is based on simulation of the missile silhouette over the pre-recorded videos of the background with fixed or moving target, is given in the paper. Coordinates of the target, read from the recorded videos of the background, are transformed to the real position of the target in the space. These target positions in function of time are input to the mathematical model of the missile movement relative to the target. The calculated coordinates of the missile are transformed to the missile silhouette position on the screen display of the flight simulator. The complete mathematical model and description of the hardware realization are given in the paper.

1. Introduction

The manual command to line-of-sight (MCLOS) guidance system of the antitank missiles requires a human operator in the guidance loop. The operator must track both the missile and the target simultaneously and guide the missile to the target. The missile is steered with a joystick, and its path is observed through a periscope-type telescopic sight. The missiles are usually equipped with a magnesium flare in the base that automatically ignites upon launch and allows the gunner to visually track the fast-moving missile.

In order to efficiently control the missile, the operator keeps the joystick in direction to minimize the missile's distance normal to the target's line-of-sight. When the distance is minimized to half, the operator has to initiate the opposite command in order to control the direction of the missile velocity [1].

The role of the man in the guidance loop has been analyzed excessively in the past. Specially designed flight simulator, for a missile's control system in which an operator controls the missile by stick while watching the target area on television, was described in [2]. A mechanical optical device, driven by an analog computer, projects the target area on a screen, which is viewed by closed-circuit TV. The concept of manual guidance of a launch vehicle from staging to orbit injection with a minimum of computation and display requirements was analyzed in [3]. The guidance scheme consists of three distinct components: computer, operator and display. This man–computer–display system enables the operator to continually generate an optimal trajectory from the vehicle's present state to the desired terminal state.

The MCLOS guidance system requires considerable training and practice for the operator since even a minor disruption in his concentration would likely cause the miss of the target. These guidance systems have limited accuracy on tank-sized targets, even with perfect line-of-sight by the operator. Therefore, this type of guidance requires a training simulator to increase the skill of the human operator and that is not only in the case of military industry but in medical neurological surgery also as presented in [4], pointing out the virtual reality concept. Applications of operator training simulator in nuclear plant and in chemical industry were shown in [5,6], giving opportunity to exercise various scenarios including accident situations.

A training flight simulator design for anti-tank combat simulation and overall CLOS missile simulation model with "6-degrees-of-freedom (6-DOF)" simulation model of short-range missiles have been presented in [7]. The image formation plane was normal to the axis of the camera and moving with the missile. The concept of the simulator treated was based on the transformation of the target position from the target plane to the image formation plane. Accuracy test for infrared search-and-track system that represents one CLOS tracking system was presented in [8] as a form of hardware-in-the-loop simulator.

* Corresponding author. Tel.: +381 11 2051707; fax: +381 65 2425041.
E-mail address: meelos.pavic@gmail.com (M. Pavic).

http://dx.doi.org/10.1016/j.ijleo.2014.06.163
0030-4026/

Modern electro-optical sensors (cameras) with reliable visual identification at ranges beyond those necessary to even detect the target with the naked eye enable modernization of the obsolete MCLOS guidance system of the antitank missiles. They are entirely passive, sensing energy emitted by target or reflected from the target. With increasing performance and decreasing cost, electro-optical systems are also used into the area of missile guidance. New generation of low-cost "inertial stabilization module (ISM)" provides integrated solution for low-cost inertial "line-of-site (LOS)" stabilization of any payload for mobile platforms including ground, air and sea. Inertial stabilization improves camera images while the camera platform is on the move. The ISM allows real-time computer control during stabilization, enabling closed-loop systems for tracking. The stabilization provided by the ISM allows for the use of higher-zoom cameras for tracking and detection systems aboard moving platforms.

These low-cost inertial LOS-stabilized cameras are used for improvement of the existing MCLOS-guided antitank missile. The operator tracks the missile and the target on the display and generates the steering commands by joystick in order to minimize the difference between the target and missile line-of-sight. The zoom law of the camera is programmed in advance in order to track efficiently the missile and the target for all target positions from minimum to maximum ranges. The sequence of width-modulated control impulses is generated on the basis of the received missile's gyro signal on reference vertical and then it is sent to the missile via the wire link.

This paper presents a new type of the training flight simulator for MCLOS guidance, based on drawing of the missile silhouette over the prerecorded videos of the background with fixed or moving target. Coordinates of the target, read from the recorded videos of the background, are transformed into the real position of the target in the space. These target coordinates in function of the time are input to the mathematical model of the missile movement relative to the target. The calculated coordinates of the missile are transformed to the missile silhouette position on the screen display of the training flight simulator. The complete mathematical model of training flight simulator of the MCLOS-guided antitank missile is given in the paper.

2. Concept of the training flight simulator

The manual command to line-of-sight guidance principle is shown in Fig. 1. The angles φ and φ_T are angular position of the missile and target line-of-sight in inertial space, respectively. The position of the missile relative to the target LOS is proportional to the angular misalignment between the missile and target line-of-sight $L = R(\varphi_T - \varphi)$, where R is the distance from the camera to the missile.

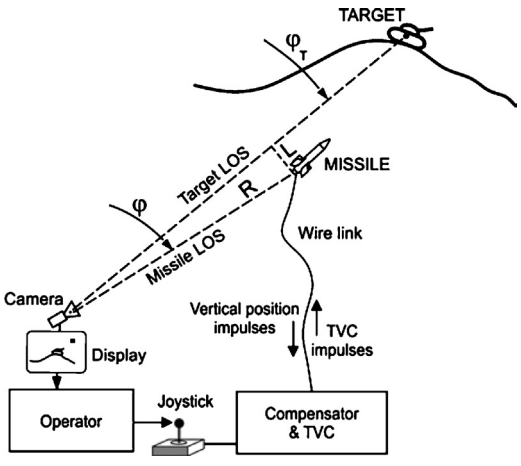

Fig. 1. Camera-supported MCLOS guidance.

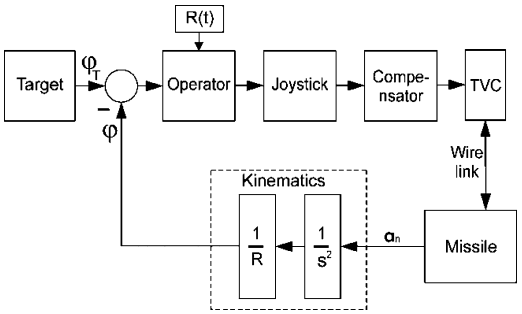

Fig. 2. Block diagram of MCLOS guidance closed-loop.

The block diagram of MCLOS guidance system is given in Fig. 2, and it is very like schematic diagram of the control structure in [9]. Since this guidance loop is unstable, it is necessary to add compensator in the guidance loop [1].

Since the concept of the training flight simulator considered in this paper is based on the video recorded by camera, the target plane is normal to the camera axis, located at the target position in the space. The simulator of the MCLOS-guided antitank missile with prerecorded videos of the background requires image formation of the missile on the target plane. The missile position relative to the line of sight is transformed to the missile projection on the target plane (Fig. 3). The target (T) and the fixed landmark (FL) are given on the target plane. The position of the line of sight relative to the inertial fixed landmark axes system $Ox_0y_0z_0$ is defined by angles χ_{LOS} and γ_{LOS}.

The training flight simulator of the manual command line-of-sight (MCLOS) antitank missile consists of:

- standalone computer,
- two displays (instructor and operator),
- operator joystick,
- data acquisition system.

The block diagram of the training flight simulator is given in Fig. 4.

The missile's steering commands from the operator joystick, being analog signals, are measured by the data acquisition system. These commands are input to the numerical simulation of the missile flight. Based on the calculated missile coordinates in the space, the missile silhouette is drawn on the display monitor over the prerecorded video.

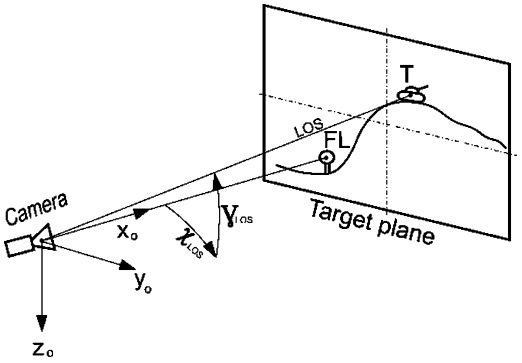

Fig. 3. Angular position of the fixed landmark and target line-of-sight.

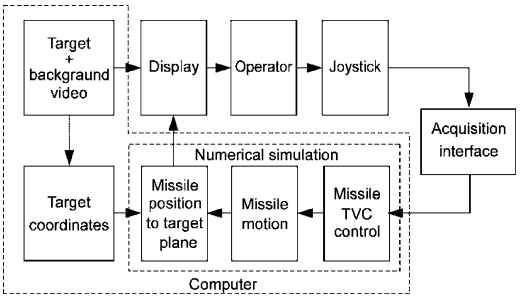

Fig. 4. Training flight simulator block diagram.

3. Processing of the video records

This type of simulator requires that the target motion remains in the plane normal to LOS. It is also necessary to know the coordinates of one fixed landmark in that plane. This landmark defines the coincidence of the video-frame to the space coordinates of the target.

3.1. Video-frame to space ratio

The space–video ratio for the recorded video is determined as a quotient of full video-frame space width at target's distance in meters and resolution of a camera's sensor in pixels. It is assumed that the space–video ratio has the same value in both plane axes, and it is determined in horizontal direction only.

The relationship between geometry in target plane and camera focal plane is shown in Fig. 5.

The camera view angle is function of focal length (Fig. 5). This function is the same in vertical and horizontal planes:

$$\alpha_H = 2 \arctan \frac{S_H}{2f} \tag{1}$$

where S_H is the horizontal length of the camera's sensor and f is the focal length of the camera's lens.

Using Eq. (1), the horizontal video-frame size in space coordinates at target's distance is determined by

$$R_H^m = 2D_T \tan \frac{\alpha_H}{2} = D_T \frac{S_H}{f} \tag{2}$$

Finally, the space–video ratio is determined by

$$R_{pix}^m = \frac{R_H^m}{R_H^{pix}} \tag{3}$$

where R_H^{pix} represents the horizontal length of the camera's sensor in pixels (camera resolution).

If camera has zooming option enabled, than the focal length is varied over time, and the space–video ratio becomes a time function.

3.2. Target coordinates

The target coordinates are read in pixels (Y_T^{pix}, Z_T^{pix}) from recorded videos in axes system AYZ fixed to the upper left corner of the video-frame (Fig. 6).

This was done manually frame-by-frame which is suitable for a limited number of training scenes, but if there was a large number of videos to process, one should use some kind of automated target detection such as presented for both color and infrared cameras [10].

A fixed landmark is chosen for orientation of the inertial axes system $Ox_0y_0z_0$, and with its coordinates in pixels (Y_{FL}^{pix}, Z_{FL}^{pix}) are read from recorded videos in axes system AYZ.

The target coordinates in that fixed landmark axes system can be determined based on the space–video ratio, having in mind that target and fixed landmark are in the same plane, and known distance to the target (D_T).

$$\begin{aligned} x_T &= D_T \\ y_T &= \left(Y_T^{pix} - Y_{FL}^{pix}\right) R_{pix}^m \\ z_T &= \left(Y_T^{pix} - Y_{FL}^{pix}\right) R_{pix}^m \end{aligned} \tag{4}$$

4. Mathematical model of the missile flight

The major missile subsystems were modeled: the vehicle dynamics, aerodynamic data, thrust vector control and compensator in the forward loop.

4.1. Missile model

The missile flight model developed in this study was a full nonlinear dynamic model with nonlinear aerodynamic data. For the purpose of MCLOS training flight simulator, the motion of a missile in space with 6-DOF is described by 12 differential equations in aeroballistics axes system $O\tilde{x}\tilde{y}\tilde{z}$, which is fixed to missile but it is not rolling with it [11]. The $O\tilde{x}$-axis of the aeroballistics system coincides with longitudinal axis of the missile directed to the tip of

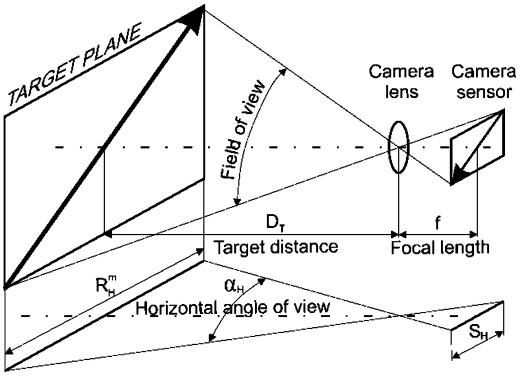

Fig. 5. Focal plane geometry.

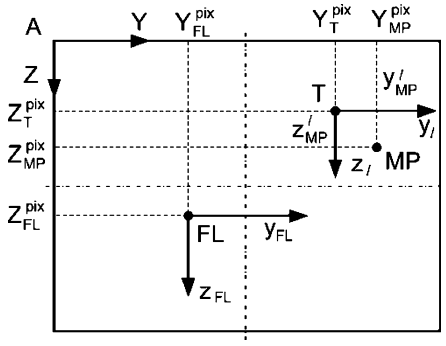

Fig. 6. Target and missile silhouette in video-frame axes system.

missile, $O\tilde{z}$-axis is in the vertical plane directed toward the Earth and $O\tilde{y}$-axis is normal to the plane$O\tilde{x}\tilde{z}$.

$$\begin{aligned}
\dot{\tilde{u}}_K &= \tilde{r}\tilde{v}_K - \tilde{q}\tilde{w}_K + \frac{\left(\tilde{X}+\tilde{F}_x\right)}{m} - g\,\sin\theta \\
\dot{\tilde{v}}_K &= p_b\tilde{w}_K - \tilde{r}\tilde{u}_K + \frac{\left(\tilde{Y}+\tilde{F}_y\right)}{m} \\
\dot{\tilde{w}}_K &= \tilde{q}\tilde{u}_K - p_b\tilde{v}_K + \frac{\left(\tilde{Z}+\tilde{F}_z\right)}{m} + g\,\cos\theta \\
\dot{p} &= \frac{\tilde{L}}{J_x} \\
\dot{\tilde{q}} &= p_b\tilde{r} - \frac{J_x}{J_y p\tilde{r}} + \frac{\left(\tilde{M}+\tilde{M}^F\right)}{J_y} \\
\dot{\tilde{r}} &= p_b\tilde{q} + \frac{J_x}{J_y p\tilde{q}} + \frac{\left(\tilde{N}+\tilde{N}^F\right)}{J_y} \\
\dot{\phi} &= p + \tilde{r}\,\tan\theta \\
\dot{\theta} &= \tilde{q} \\
\dot{\psi} &= \frac{\tilde{r}}{\cos\theta} \\
\dot{x} &= \tilde{u}_K\,\cos\theta\cos\psi - \tilde{v}_K\sin\psi + \tilde{w}_K\sin\theta\cos\psi \\
\dot{y} &= \tilde{u}_K\,\cos\theta\sin\psi + \tilde{v}_K\cos\psi - \tilde{w}_K\sin\theta\sin\psi \\
\dot{h} &= -\dot{z} = \tilde{u}_K\,\sin\theta - \tilde{w}_K\cos\theta
\end{aligned} \tag{5}$$

where $\tilde{u}_K$, $\tilde{v}_K$, $\tilde{w}_K$ are the components of the missile velocity V_K relative to the Earth in the aeroballistics axes system, $\tilde{p}$, $\tilde{q}$, $\tilde{r}$ are the roll, pitch and yaw rates in the aeroballistics axes system, respectively, ϕ, θ, ψ are the roll, pitch and azimuth angle, respectively, and x, y, z are the coordinates of the missile position in the Earth-fixed reference frame (inertial system), respectively.

The component of the angular rate of the aeroballistics axes system in the $O\tilde{x}$-direction is given by

$$p_b = -\tilde{r}\,\tan\theta \tag{6}$$

The aerodynamic force components along the three body axes are represented by $\tilde{X}$, $\tilde{Y}$, $\tilde{Z}$ in terms of the aerodynamic coefficients:

$$\begin{aligned}
\tilde{X} &= \tilde{C}_x QS \\
\tilde{Y} &= \tilde{C}_y QS \\
\tilde{Z} &= \tilde{C}_z QS \\
Q &= \frac{\rho V^2}{2}
\end{aligned} \tag{7}$$

where ρ being the air density, V the missile velocity relative to the air, $S = \pi d^2/4$ the reference area and Q the dynamic pressure. Alternative symbols are for the axial force $\tilde{C}_A = -\tilde{C}_X$, and for the normal force $\tilde{C}_N = -\tilde{C}_Z$.

The components of the aerodynamic moment about the body axes are defined as rolling moment ($\tilde{L}$), pitching moment ($\tilde{M}$) and yawing moment ($\tilde{N}$) in terms of the corresponding coefficients $\tilde{C}_l$,$\tilde{C}_m$ and $\tilde{C}_n$:

$$\begin{aligned}
\tilde{L} &= \tilde{C}_l QSl \\
\tilde{M} &= \tilde{C}_m QSl \\
\tilde{N} &= \tilde{C}_n QSl
\end{aligned} \tag{8}$$

where l is the reference length, usually $l = d$.

The following form of the force and moment coefficients are used in this study:

$$\begin{aligned}
\tilde{C}_A &= \tilde{C}_{Ao} + \tilde{C}_{A_2}\left(\tilde{\alpha}^2 + \tilde{\beta}^2\right) \\
\tilde{C}_N &= \tilde{C}_{N\alpha}\cdot\tilde{\alpha} + \tilde{C}_{Nq}\cdot\tilde{q}^* \\
\tilde{C}_Y &= -\tilde{C}_{N\alpha}\cdot\tilde{\beta} + \tilde{C}_{Nq}\cdot\tilde{r}^* \\
\tilde{C}_l &= \tilde{C}_{lo} + \tilde{C}_{lp}\tilde{p}^* \\
\tilde{C}_m &= \tilde{C}_{m\alpha}\cdot\tilde{\alpha} + \tilde{C}_{mq}\cdot\tilde{q}^* \\
\tilde{C}_n &= -\tilde{C}_{m\alpha}\cdot\tilde{\beta} + \tilde{C}_{mq}\cdot\tilde{r}^*
\end{aligned} \tag{9}$$

The angular velocities are normalized by V/l:

$$\tilde{p}^* = \frac{\tilde{p}\cdot l}{V}, \quad \tilde{q}^* = \frac{\tilde{q}\cdot l}{V}, \quad \tilde{r}^* = \frac{\tilde{r}\cdot l}{V} \tag{10}$$

All derivatives of the force and moment coefficients in Eqs. (9) are the functions of the Mach number.

In the above equations, the aerodynamic forces and moments are calculated for the missile velocity relative to the air:

$$\begin{aligned}
\begin{bmatrix}\tilde{u}\\ \tilde{v}\\ \tilde{w}\end{bmatrix} &= \begin{bmatrix}\tilde{u}_K\\ \tilde{v}_K\\ \tilde{w}_K\end{bmatrix} - \begin{bmatrix}\tilde{u}_w\\ \tilde{v}_w\\ \tilde{w}_w\end{bmatrix} \\
V &= \sqrt{\tilde{u}^2 + \tilde{v}^2 + \tilde{w}^2}
\end{aligned} \tag{11}$$

Having in mind the components of the wind velocity in the Earth axes system, we can determine its components in the aero-ballistic axes system:

$$\begin{bmatrix}\tilde{u}_W\\ \tilde{v}_W\\ \tilde{w}_W\end{bmatrix} = C\left(\psi,\theta,0\right)\begin{bmatrix}w_x\\ w_y\\ 0\end{bmatrix} \tag{12}$$

where C is the transformation matrix [6].

Now we can determine the angle of attack and angle of side slip in aero-ballistic reference frame required in Eq. (9):

$$\tilde{\alpha} = \frac{\tilde{w}}{V}, \quad \tilde{\beta} = \frac{\tilde{v}}{V} \tag{13}$$

4.2. Joystick

Based on the angular difference between the target and missile line-of-sight, the operator generates the commands by joystick in two perpendicular directions (η_j, ζ_j). The command in one direction corresponds to the vertical plane of the missile flight (η_j) and the second one to the horizontal plane (ζ_j).

A 2-DOF magneto-rheological actuator joystick was presented in [12] and in the guidance loop of the training flight simulator, similar joystick was used with the same spherical angle measurement principle but without force feedback actuators. Its static characteristics obtained by measurement of command coefficients for given angular deflections are shown in Fig. 7 for horizontal and vertical planes.

The commands generated by the operator are nonlinear functions of the joystick deflections. The nonlinear characteristics of the joystick can be represented by two slopes. The lower gradient slopes are in the range -12° to 12° of the joystick deflection in the horizontal plane, and -20° to 20° in the vertical plane. These lower gradients permit the operator to achieve better control of the missile when the missile is close to the line-of-sight. The second slopes, with higher gradient, are on the other side of these boundaries to the maximum of $\pm 22^\circ$ in the horizontal plane, and $\pm 35^\circ$ in the vertical plane.

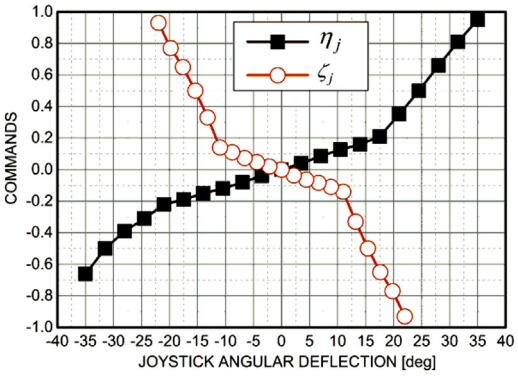

Fig. 7. Static characteristics of the joystick.

The diagram of the command in function of joystick deflections is symmetrical in horizontal plane, while in vertical plane it is asymmetrical. The maximal positive (upward) command is equal to unity $\eta_j = 1$, while the maximal negative (downward) command is $\eta_j = -0.65$. This limitation of the maximal negative command is used to prevent accidental excessive downward commands, since the missile flight path is close to the ground.

4.3. Compensator

Instead of using the operator's intelligence to supply the necessary amount of phase advance, the stability of the guidance loop of the command to line-of-sight guidance is realized by differential compensator in the forward loop (phase lead compensator). Since the same type of the compensator is used for both vertical and horizontal planes, only the pitch channel compensator is considered here:

$$\frac{\eta_c}{\eta_j} = \frac{T_d s + 1}{T_i s + 1} \tag{14}$$

The output of the compensator can be written in the canonical form:

$$\begin{aligned} \eta_c &= \eta_c' + \frac{T_d}{T_i}\eta_j \\ \dot{\eta}_c' &= -\frac{1}{T_i}\eta_c' + \frac{\left(1 - T_d/T_i\right)}{T_i}\eta_j \end{aligned} \tag{15}$$

where η_c' is the auxiliary state variable.

The thrust vector steering commands (η^F, ζ^F) are obtained by adding the compensation of the gravity (η_g) to the vertical component of the commands at the output of the compensator.

$$\begin{aligned} \eta^F &= \eta_c + \eta_g \\ \zeta^F &= \zeta_c \end{aligned} \tag{16}$$

4.4. Trust vector control

The missile treated in this paper is controlled by trust vector width-modulated control impulses. Fig. 8 shows the typical variation of lateral jet force during one revolution of missile when the control surface can take only two positions [13]. Hence, the lateral force takes only two values $\pm F_0$. The mean values of lateral jet forces along horizontal and vertical directions can be determined using notation in Fig. 8:

$$\begin{aligned} \tilde{F}_y &= \zeta^F F_{max} \\ \tilde{F}_z &= -\eta^F F_{max} \end{aligned} \tag{17}$$

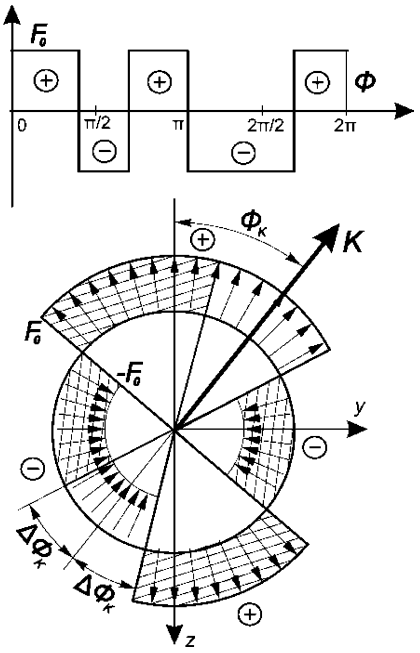

Fig. 8. Width-modulated control impulse.

where F_{max} is the maximal mean value of lateral jet force during one revolution of the missile

$$F_{max} = \frac{2}{\pi}F_0 \tag{18}$$

Using the notation in Fig. 8, one can obtain the relations between rectangular (ζ^F, η^F) and polar (K, Φ_K) coordinates of command coefficient for the given sequence of width-modulated control impulses:

$$\zeta^F = K \sin \Phi_K, \quad \eta^F = \cos \Phi_K \tag{19}$$

where the total command coefficient is given as the ratio of the mean to the maximal mean value of the lateral jet force during one rotation of missile:

$$K = \frac{F_{mean}}{F_{max}} = \sin \Delta\Phi_K \tag{20}$$

The mean values of lateral jet moments are:

$$\begin{aligned} \tilde{M}^F &= \tilde{F}_z\left(l_{TVC} - l_{CM}\right) \\ \tilde{N}^F &= -\tilde{F}_y\left(l_{TVC} - l_{CM}\right) \end{aligned} \tag{21}$$

where l_{TVC} and l_{CM} determine the jet force and center of mass positions from the apex of the missile, respectively.

4.5. Missile position relative to the target LOS

The line-of-sight of the target is defined by angles χ_{LOS} and γ_{LOS} relative to the inertial axes system ($Ox_0y_0z_0$). Using target's coordinates in inertial system (Fig. 3), we get

$$\begin{aligned} \chi_{LOS} &= \tan^{-1}\frac{y_T}{x_T} \\ \gamma_{LOS} &= -\sin^{-1}\frac{z_T}{\sqrt{x_T^2 + y_T^2 + z_T^2}} \end{aligned} \tag{22}$$

$$\begin{bmatrix} x_l \\ y_l \\ z_l \end{bmatrix} = C\left(\chi_{LOS}, \gamma_{LOS}, 0\right) \begin{bmatrix} x \\ y \\ z \end{bmatrix} \tag{23}$$

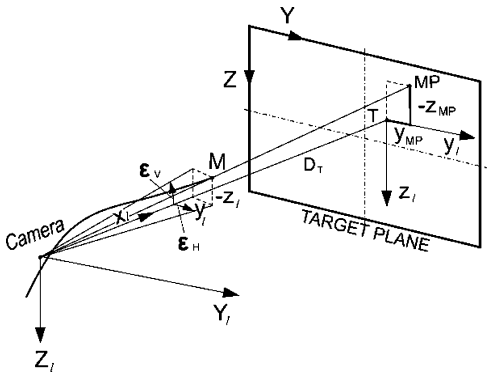

Fig. 9. Missile position relative to the target LOS.

The position of the missile line-of-sight relative to the target line-of-sight (LOS) is defined by angles ε_H and ε_V in Fig. 9.

$$\varepsilon_V = -\tan^{-1}\frac{z_l}{x_l}$$
$$\varepsilon_H = \tan^{-1}\frac{y_l}{x_l} \quad (24)$$

The coordinates of the projected position of the missile (MP) on the target plane are function of the known distance to the target (D_T).

$$y^l_{MP} = D_T \tan \varepsilon_H$$
$$z^l_{MP} = -D_T \tan \varepsilon_V \quad (25)$$

4.6. Missile silhouette coordinates

Since the target coordinates in pixels are known (X^{pix}_T, X^{pix}_T), the coordinates of the missile silhouette (missile projected point) in video-frame axes system can be determined from the coordinates of the missile projected point in line-of-sight axes system (Fig. 9):

$$Y^{pix}_{MP} = Y^{pix}_T + \frac{y^l_{MP}}{R^m_{pix}}$$
$$Z^{pix}_{MP} = Z^{pix}_T + \frac{z^l_{MP}}{R^m_{pix}} \quad (26)$$

5. Software realization and numerical example

The training flight simulator software is developed in Microsoft Visual Basic 6, and Microsoft Access 2007 is used for the database. In order to avoid afterward changes in user interface discussed in [14], all members of the training crew were taken part in the user interface design process.

The instructor's display presentation of the combat simulation of the missile guidance against the fixed target (bunker) and the missile silhouette presentation over the prerecorded video is given in Fig. 10.

The training options are shown on the instructor's display. These options are: operator in training session, types of camera (day/night), fixed or moving target and launcher platform, propellant temperature, wind (constant or turbulent) defined by its magnitudes in axial and lateral directions, and initial missile entrance into the camera field of view (deterministic or stochastic). If the deterministic option is selected, the instructor can choose one of the nine available entrance directions. The trajectory graph button is for analysis of the guidance quality, and finally options for maintenance of the database tables.

The video of the fixed target located 2000 m from the launcher is taken as an illustration of one successful training exercise. The

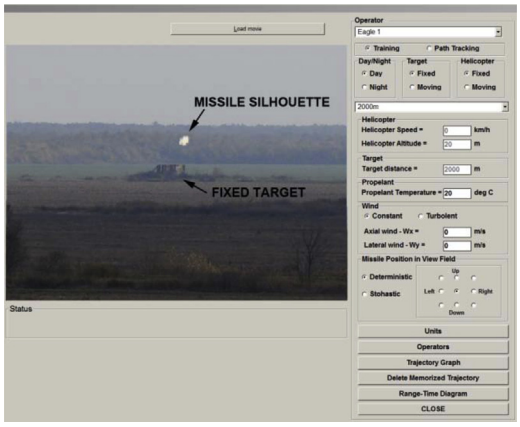

Fig. 10. Instructor's display of the combat simulation.

missile was launched at the altitude of 20 m with the elevation of 4° relative to the target line-of-sight. The lateral position of the missile relative to the line-of-sight in horizontal plane was 3.5 m and the missile was directed to cross the line-of-sight at the down-range of 50 m. The guidance of the missile started after ballistic flight of 0.7 s.

The vertical and horizontal projections of the missile trajectory are given in Fig. 11, and one should note that in vertical plane bunker silhouette is about 3 m high, and operator was hit the center of the target.

The commands used for missile steering are given in Fig. 12. These commands are composed of the commands generated by the operator and compensation of the gravity. It can be seen from Fig. 12 that first 500 m there is almost no commands generated by the operator in vertical plane, but there is only parts of the commands for compensation of the gravity. In the same interval, there

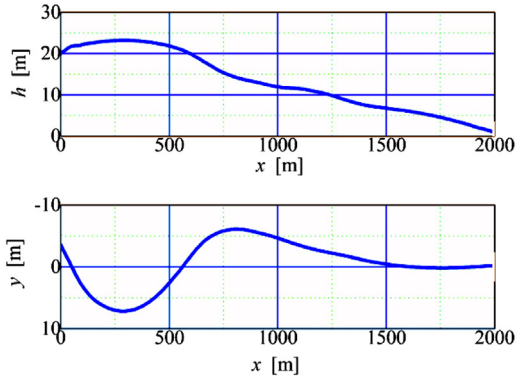

Fig. 11. Missile trajectory in vertical and horizontal planes.

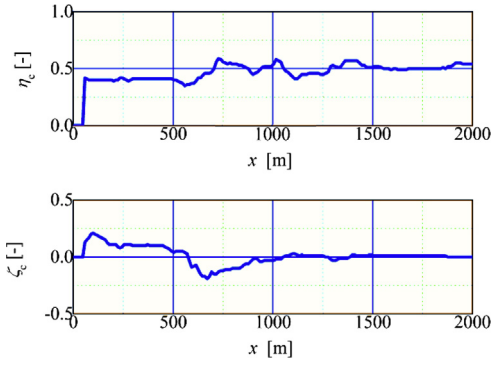

Fig. 12. Guidance commands in vertical and horizontal planes.

are commands generated by the operator in horizontal plane to bring missile to the line-of-sight.

6. Conclusions

The obsolete MCLOS guidance system of antitank missiles was improved by modern electro-optical cameras which enables the operator to spot and track the target and the missile on the monitor display and generates the steering commands by joystick in order to minimize the difference between the target and the missile line of sight.

This modernized MCLOS guidance system of antitank missiles requires a new type of training simulator. The training flight simulator presented in this paper is in fact hardware in the loop simulator where the joystick and the display are hardware part of the simulator and they are identical as in real combat system. In this way, operator training is more efficient and more like real combat situations where besides missile guidance training he is trained for target spotting and recognition in real scenes.

Unlike any other, the presented simulator covers the prerecorded videos of the background with fixed or moving target and numerical simulation of the missile flight (based on the six-degrees-of-freedom mathematical model) and the missile control system. Since the analyzed missile is controlled by trust vector control, the mathematical model of the relation between the mean values of lateral jet force and the command generate by joystick are given in the paper.

Based on the calculated position of the missile in the space, the position of the missiles silhouette in the video frame is determined and novelty presented in this paper is geometry coordinate transformation with fixed landmark in inertial space which enables the use of non-stabilized color/infrared cameras.

The developed training simulator enables analysis of the different type of real disturbances to the operator capabilities to adequately react. Disturbances covered by software are: propellant temperature, wind and launcher position. The flexibility of the software enables to add some another type of disturbances, easily. The initial results are great. The experienced operators confirmed that missile behavior is like in reality in a field, and new operators now have an ability to train in the classroom before shooting the real missiles. The results for each of the numerical simulation are stored in the computer memory which enables analysis of the operator skill. The diagrams of the missile trajectory and generated commands for one of the training simulation are given in the paper.

References

[1] P. Garnel, D.J. East, Guided Weapon Control System, 2nd ed., Pergamon Press, Oxford, 1980.
[2] P.L. Lopresti, TV missile terminal-flight simulator, J. Spacecraft Rockets (1964) 438–444.
[3] J.D. Gilchrist, A manual optimal guidance scheme using a predictive model, J. Spacecraft Rockets (1968) 1181–1187.
[4] P.J. Schmitt, N.C.J. Agarwal, From planes to brains – parallels between military development of virtual reality environments and virtual neurological surgery, World Neurosurg. (2012) 214–219.
[5] T. Jayanthi, H. Seetha, K.R.S. Narayanan, N. Jasmine, R. Nawlakha, B. Sankar, J. Chakraborty, S.A.V. SatyaMurty, P. Swaminathan, Simulation and integrated testing of process models of PFBR operator training simulator, Energy Procedia (2011) 653–659.
[6] S. Brambilla, D. Manca, Recommended features of an industrial accident simulator for the training of operators, J. Loss Prev. Process Industries (2011) 344–355.
[7] G.M. Dimirovski, D.D. Mohenski, S.M. Deskovski, A Simulator for line-of-sight missile control and guidance systems: object-oriented design, Proc. IEEE Aerospace Conf. (2003) 2809–2822.
[8] H.M. Qu, D. Cao, Q. Zheng, Y.Y. Li, Q. Chen, Accuracy test and analysis for infrared search and track system, Optik 124 (2013) 2313–2317.
[9] J. Zhou, Z. Jiang, H. Li, Investigation into pilot handling qualities in teleoperation rendezvous and docking with time delay, Chin. J. Aeronaut. (2012) 622–630.
[10] T.L. Weng, Y.Y. Wang, Z.Y. Ho, Y.N. Sun, Weather-adaptive flying target detection and tracking from infrared video sequences, Expert Syst. Appl. (2010) 1666–1675.
[11] B. Etkin, L.D. Reid, Dynamics of Flight Stability and Control, 3rd ed., Wiley, 1996, pp. 93–128.
[12] W.H. Li, B. Liu, P.B. Kosasih, X.Z. Zhang, A 2-DOF MR actuator joystick for virtual reality applications, Sens. Actuators A (2007) 308–320.
[13] D. Cuk, Characteristics of impulse control of canard missile, Sci. Tech. Rev. (1983) 11–18 (in Serbian).
[14] R.J. Branaghan, C.M. Covas-Smith, K.D. Jackson, C. Eidman, Using knowledge structures to redesign an instructor-operator station, Appl. Ergon. (2011) 934–940.